DOI: 10.1002/chem.200700206

Aromaticity: Molecular-Orbital Picture of an Intuitive Concept

Simon C. A. H. Pierrefixe and F. Matthias Bickelhaupt*[a]

Dedicated to Professor Roald Hoffmann on the occasion of his 70th birthday

Abstract: Geometry is one of the primary and most direct indicators of aromaticity and antiaromaticity: a regular structure with delocalized double bonds (e.g., benzene) is symptomatic of aromaticity, whereas a distorted geometry with localized double bonds (e.g., 1,3-cyclobutadiene) is characteristic of antiaromaticity. Here, we present a molecular-orbital (MO) model of aromaticity that explains, in terms of simple orbital-overlap arguments, why this is so. Our MO model is based on accurate Kohn–Sham DFT analyses of the bonding in benzene, 1,3-cyclobutadiene, cyclohexane, and cyclobutane, and how the bonding mechanism is affected if these molecules undergo geometrical deformations between regular, delocalized ring structures, and distorted ones with localized double bonds. We show that the propensity of the π electrons is always, that is, in both the aromatic and antiaromatic molecules, to localize the double bonds, against the delocalizing force of the σ electrons. More importantly, we show that the π electrons nevertheless decide about the localization or delocalization of the double bonds. A key component of our model for uncovering and resolving this seemingly contradictory situation is to analyze the bonding in the various model systems in terms of two interpenetrating fragments that preserve, in good approximation, their geometry along the localization/delocalization modes.

Keywords: aromaticity · benzene · bond theory · cyclobutadiene · density functional calculations

Introduction

Ever since the early work of Kékulé in the mid 19th century, benzene (**1**) and its aromatic nature have appealed to the imagination of generations of chemists and physicists.[1]

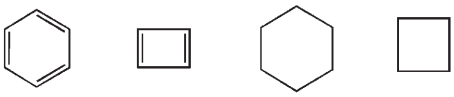

1 2 3 4

The concept of aromaticity is to some extent intuitive. The core of aromatic nature is often defined by referring to a series of structural, energetic, and spectroscopic characteristics, of which the following constitute the core: 1) a highly symmetric, delocalized structure involving six C–C bonds of equal length, each with partial double-bond character, 2) enhanced thermodynamic stability, and 3) reduced reactivity relative to nonaromatic conjugated hydrocarbons.[2] Other properties that have been taken as symptoms of aromatic character are, for example, the downfield shift in proton NMR spectra, the exaltation of diamagnetic susceptibility, and a comparatively low reactivity.[3–5] The counterpart of **1** is the antiaromatic 1,3-cyclobutadiene (**2**), which, for example, shows localized double bonds instead of a regular delocalized structure with four C–C bonds of equal length.[2]

Aromaticity continues to be a topic in many studies associated not only with its relevance in chemistry, biology, and technology, but also with the very concept itself.[5,6] Indeed, despite many pioneering contributions on this issue, there is still a gap in our physical understanding of the nature of aromaticity.[2–7] In the early 20th century, Pauling and Hückel were the first to quantum chemically address the issue of benzene's (**1**) structure and enhanced stability by using valence-bond (VB) and molecular-orbital (MO) theory.[8,9] In a VB-type approach, used by both Pauling and Hückel, the circular topology of benzene enables a resonance between the wavefunctions of two complementary sets of localized

[a] S. C. A. H. Pierrefixe, Dr. F. M. Bickelhaupt
Afdeling Theoretische Chemie
Scheikundig Laboratorium der Vrije Universiteit
De Boelelaan 1083, NL-1081 HV Amsterdam (The Netherlands)
Fax: (+31) 20-598-7629
E-mail: FM.Bickelhaupt@few.vu.nl

Supporting information for this article is available on the WWW under http://www.chemeurj.org/ or from the author.

bonds, leading to an additional stabilization. In the MO approach applied by Hückel to the benzene problem, the enhanced stability of **1** relative, for example, to isolated or linearly conjugated double bonds, is attributed to an extra bonding contact (or resonance integral or interaction matrix element) in circularly conjugated hydrocarbons with $4n+2$ π electrons[9] (a generalization to other than pericyclic topologies was later derived by Goldstein and Hoffmann).[10] The driving force for delocalization in **1** and other circularly conjugated $4n+2$ π-electron species and, likewise, the tendency of **2** and other circularly conjugated $4n$ π-electron systems to form localized double bonds was, therefore, originally attributed to the π-electron system ($n=1$ for **1** and **2**).[4]

Herein, we address the question of why **1** and **2** have delocalized and localized structures, respectively, that is, with six equivalent C–C bonds in **1** and with alternating single and double bonds in **2**. Recent sophisticated VB[11,12] as well as MO studies[13] confirm that the circular conjugation in benzene's π-electron system is responsible for this molecule's enhanced stability. This is also reproduced by our calculations and will not be further discussed here. On the other hand, since the late 1950s, evidence has been repeatedly reported that refutes the idea that benzene's (**1**) D_{6h} symmetric structure originates from a delocalizing propensity of its π-electron system.[14,15] This led to the somewhat contradictory notion, nicely sketched by Kutzelnigg,[16] that, on the one hand, benzene's regular, delocalized structure is only possible due to the π electron's capability to form delocalized bonds and, on the other hand, the very same π electrons do favor a structure with localized double bonds. The distortive propensity of the π electrons has been confirmed in various studies during the last two decades.[15] Evidence comes not only from theory but also from experiment, such as benzene's surprisingly low-energy and large-amplitude B_{2u} bond-alternation mode observed by Berry already in 1961.[14e] This interpretation has been supported more recently by Haas and Zilberg's (computational) observation of an increase in the frequency of this B_{2u} bond-alternation mode as benzene undergoes $\pi\rightarrow\pi^*$ excitation from ground to first-excited state.[15a] Shaik, Hiberty, and co-workers[11] showed, in terms of an elegant VB model, that it is the σ system that enforces the delocalized, D_{6h} symmetric structure of **1** upon the π system, which intrinsically strives for localized double bonds. These conclusions initiated a debate,[17] but were eventually reconfirmed by others.[13,18] One factor that promoted a controversy is that, whereas in VB theory there is a clear model to explain why, for example, in **1** σ delocalization overrules π localization, such a clear model is missing in MO theory, despite that fact that initially the MO model played such an important role in the question on aromatic stabilization and, beyond this particular issue, has been enormously successful in clarifying chemistry in general.[19]

Our purpose is to develop a simple, qualitative MO model, based on accurate computations, that explains why benzene (**1**) shows delocalized double bonds, whereas 1,3-cyclobutadiene (**2**) features localized double bonds. Apart from arriving at a better understanding of these archetypal geometric symptoms of aromaticity and antiaromaticity, this closes a gap in the MO theoretical treatment of this issue. Thus, we have quantum chemically investigated **1**, **2**, planar cyclohexane (**3**) and planar cyclobutane (**4**) at the BP86/TZ2P level of density functional theory (DFT) by using the Amsterdam Density Functional (ADF) program.[20]

Our MO model reveals that in both the aromatic and antiaromatic model compounds, the π-electron system always has a propensity to localize double bonds, against the delocalizing force of the σ-electron system. Interestingly, we can also resolve the seemingly contradictory notion that, despite the fact that they have in all cases a distortive, localizing propensity, the π electrons play a decisive role in determining that benzene can adopt its delocalized aromatic structure, whereas cyclobutadiene obtains a localized antiaromatic structure. From our MO model, this can be understood in terms of simple orbital-overlap arguments.

Abstract in French: *La géométrie d'un système moléculaire est l'un des indicateurs premiers et évidents de son aromaticité ou de son antiaromaticité. Par exemple, une structure symétrique présentant des doubles liaisons délocalisées comme le benzène est caractéristique d'aromaticité alors qu'une géométrie distordue qui montre des doubles liaisons localisées comme le 1,3-cyclobutadiène est typique d'antiaromaticité. Dans ce travail, nous présentons un modèle de l'aromaticité basé sur le formalisme d'orbitales moléculaires (OM), qui explique pourquoi il en est ainsi en utilisant uniquement des notions de recouvrement orbitalaire. Notre modèle d'OM est basé sur des analyses de la liaison à l'aide de calculs Kohn–Sham DFT dans le benzène, le 1,3-cyclobutadiène, le cyclohexane et le cyclobutane. L'accent a notamment été mis sur l'étude de l'influence des déformations structurales pour passer d'un système symétrique délocalisé à un système localisé à géométrie distordue sur le mode de liaison de ces molécules. Nous montrons que les électrons π cherchent systématiquement à localiser les doubles liaisons aussi bien dans les molécules aromatiques que dans les systèmes antiaromatiques, et ce contre la tendance à la délocalisation des électrons σ. Il est montré de plus que le système π gouverne toujours la localisation ou délocalisation des doubles liaisons. L'élément clé de notre modèle pour résoudre cette situation a priori contradictoire est l'analyse de la liaison sur la base de l'interaction entre deux fragments qui conservent leurs géométries aussi bien dans les systèmes localisés et délocalisés.*

Theoretical Methods

General procedure: All calculations were performed by using the Amsterdam Density Functional (ADF) program developed by Baerends and others.[20] The numerical integration was performed by using the procedure developed by te Velde et al.[20g,h] The MOs were expanded in a large uncontracted set of Slater-type orbitals (STOs) containing diffuse functions: TZ2P (no Gaussian functions are involved).[20i] The basis set is of

triple-ζ quality for all atoms and was augmented with two sets of polarization functions, that is, 3*d* and 4*f* on C and 2*p* and 3*d* on H. The 1*s* core shell of carbon were treated by the frozen-core approximation.[20c] An auxiliary set of *s*, *p*, *d*, *f*, and *g* STOs was used to fit the molecular density and to represent the Coulomb and exchange potentials accurately in each self-consistent field cycle.[20j]

Equilibrium structures were optimized by using analytical gradient techniques.[20k] Geometries and energies were calculated at the BP86 level of the generalized gradient approximation (GGA): exchange is described by Slater's Xα potential[20l] with corrections due to Becke[20m,n] added self-consistently and correlation is treated in the Vosko–Wilk–Nusair (VWN) parameterization[20o] with nonlocal corrections due to Perdew[20p] added, again, self-consistently (BP86).[20q]

Bonding-energy analysis: To obtain more insight into the nature of the bonding in our aromatic (**1**), antiaromatic (**2**), and nonaromatic model systems (**3**, **4**), an energy decomposition analysis was carried out.[21] In this analysis, the total binding energy ΔE associated with forming the overall molecular species of interest, say AB, from two (or sometimes more) radical fragments, A′+B′, is made up of two major components [Eq. (1)]:

$$\Delta E = \Delta E_{prep} + \Delta E_{int} \quad (1)$$

In this formula, the preparation energy ΔE_{prep} is the amount of energy required to deform the individual (isolated) radical fragments from their equilibrium structure (A′, B′) to the geometry that they acquire in the overall molecule (A, B). The interaction energy ΔE_{int} corresponds to the actual energy change when these geometrically deformed fragments A and B are combined to form the combined molecular species AB. It is analyzed in the framework of the Kohn–Sham molecular-orbital (MO) model by using a quantitative decomposition of the bond into electrostatic interaction, Pauli repulsion (or exchange repulsion or overlap repulsion), and (attractive) orbital interactions [Eq. (2)]:[21]

$$\Delta E_{int} = \Delta V_{elstat} + \Delta E_{Pauli} + \Delta E_{oi} \quad (2)$$

The term ΔV_{elstat} corresponds to the classical electrostatic interaction between the unperturbed charge distributions $\rho_A(r)+\rho_B(r)$ of the prepared or deformed radical fragments A and B (see below for definition of the fragments) that adopt their positions in the overall molecule AB, and is usually attractive. The Pauli repulsion term ΔE_{Pauli} comprises the destabilizing interactions between occupied orbitals and is responsible for the steric repulsion. This repulsion is caused by the fact that two electrons with the same spin cannot occupy the same region in space. It arises as the energy change associated with the transition from the superposition of the unperturbed electron densities $\rho_A(r)+\rho_B(r)$ of the geometrically deformed but isolated radical fragments A and B to the wavefunction $\Psi^0 = N\hat{A}\,[\Psi_A\,\Psi_B]$, that properly obeys the Pauli principle through explicit antisymmetrization ($\hat{A}$ operator) and renormalization (N constant) of the product of fragment wavefunctions (see Ref. [21a] for an exhaustive discussion). The orbital interaction ΔE_{oi} in any MO model, and, therefore, also in Kohn–Sham theory, accounts for electron-pair bonding,[21a,b] charge transfer (i.e., donor–acceptor interactions between occupied orbitals on one moiety with unoccupied orbitals of the other, including the HOMO–LUMO interactions), and polarization (empty–occupied orbital mixing on one fragment due to the presence of another fragment). In the bond-energy decomposition, open-shell fragments are treated with the spin-unrestricted formalism, but, for technical (not fundamental) reasons, spin polarization is not included. This error causes an electron-pair bond to become too strong in the order of a few kcal mol^{-1}. To facilitate a straightforward comparison, the results of the energy decomposition were scaled to match exactly the regular bond energies. Because the Kohn–Sham MO method of DFT in principle yields exact energies and, in practice, with the available density functionals for exchange and correlation, rather accurate energies, we have the special situation that a seemingly one-particle model (a MO method) in principle completely accounts for the bonding energy.[21a]

The orbital-interaction energy can be decomposed into the contributions from each irreducible representation Γ of the interacting system [Eq. (3)] by using the extended transition-state (ETS) scheme developed by Ziegler and Rauk[21c–e] (note that our approach differs in this respect from the Morokuma scheme,[22] which instead attempts a decomposition of the orbital interactions into polarization and charge transfer):

$$\Delta E_{oi} = \Sigma_\Gamma \Delta E_\Gamma = \Delta E_\sigma + \Delta E_\pi \quad (3)$$

In our model systems, the irreducible representations can be categorized into symmetric and antisymmetric with respect to the mirror plane provided by the carbon-atom framework, which correspond to what is commonly designated σ- and π-electron systems, respectively. This gives rise to the orbital-interaction components ΔE_σ and ΔE_π, as shown in Equation (3) above.

Results and Discussions

First, we focus on benzene (**1**) and 1,3-cyclobutadiene (**2**) for which we find the usual D_{6h} and D_{2h} symmetric equilibrium geometries: **1** has six equivalent C–C bonds of 1.398 Å and **2** has alternating short and long bonds of 1.338 and 1.581 Å (see Scheme 1). To understand why **1** opposes to localization and **2** undergoes localization, we have examined the energy and bonding of these species along a distortion mode proceeding from a regular delocalized structure with all C–C bonds equivalent towards a geometry with alternating single and double bonds. A key step in our approach is that this can be done by rotating two equivalent and geometrically frozen fragments relative to each other, as shown in Scheme 1, which greatly reduces the complexity of the bond analysis because we go from a multi-fragment to a two-fragment problem. For benzene, we go from D_{6h} symmetric **1** with all C–C bonds at 1.398 Å to a D_{3h} symmetric structure with alternating C–C bonds of 1.291 and 1.502 Å. For comparison, the C–C bond lengths in ethylene and ethane are, at the same level of theory, 1.333 and 1.532 Å. In the case of cyclobutadiene, we go from a D_{4h} symmetric species with all C–C bonds at 1.465 Å to the D_{2h} symmetric **2** with alternating C–C bonds of 1.338 and 1.581 Å. Note

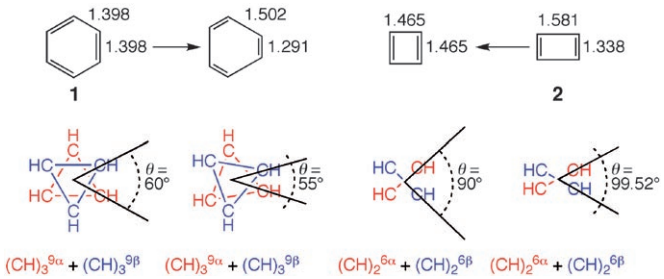

Scheme 1. Construction and distortion of **1** and **2** in terms of two rigid fragments.

that along this distortion of cyclobutadiene, we preserve the singlet electron configuration of the equilibrium structure **2**, as we wish to understand the behavior of the latter (the D_{4h} arrangement has a triplet ground state that is 5.19 kcal mol^{-1} above **2** and has C–C bonds of 1.444 Å).

At this point, we note that, although physically quite plausible, our choices of deformation modes, in particular the nonequilibrium localized benzene and delocalized 1,3-cyclobutadiene geometries, are not unique. We have, therefore, verified that all trends and conclusions that play a role in the following discussion are not affected if other plausible choices are made. Thus, we have analyzed the bonding in benzene, analogously to the procedure defined in Scheme 1, but proceeding from a localized benzene structure with alternating C–C distances of 1.333 and 1.532 Å, that is, the C–C bond lengths in ethene and ethane (the corresponding delocalized structure has C–C distances of 1.434 Å). Likewise, we repeated our analyses for 1,3-cyclobutadiene by proceeding from the delocalized equilibrium geometry of the triplet ground state with equal C–C bonds of 1.444 Å (the corresponding localized geometry has alternating C–C bonds of 1.319 and 1.559 Å). The results for this alternative choice of deformation mode, which are shown in Figure S1 and Table S1 of the Supporting Information, fully reproduce and confirm all trends and conclusions that we obtain with the definition of Scheme 1 (shown in Figures 1 and 2 and Table 1). The same holds also for yet another plausible choice for a cyclohexatriene-like benzene structure with alternating C–C bonds of 1.330 and 1.480 Å that correspond to the single and double bonds in 1,3-butadiene (results not shown). We conclude that, whereas the precise numerical values vary somewhat, the trends that are essential for our conclusions are quite robust regarding the exact choice of the deformation mode.

Now we return to the discussion of our analyses of the deformation modes defined in Scheme 1. In our approach, the change in energy ΔE that goes with localizing our model systems is equal to the change in interaction energy ΔE_{int} between two geometrically frozen $(CH)_3^{9\bullet}$ fragments in their decet valence configuration for benzene and two $(CH)_2^{6\bullet}$ fragments in their septet valence configuration for cyclobutadiene. The preparation energy ΔE_{prep} vanishes in this analysis because it is constant for geometrically frozen fragments. Each pair of fragments has mutually opposite spins (superscripts α and β in Scheme 1) to allow for the formation of all σ- and π-electron-pair bonds. These $(CH)_3^{9\bullet}$ and $(CH)_2^{6\bullet}$ fragments are weakly (relative to the bonding interactions in **1** and **2**) repulsive conglomerates of three and two $CH^{\bullet\bullet\bullet}$ radicals, respectively (see also Table 1). The changes in interaction can be analyzed within the conceptual framework of the MO model contained in Kohn–Sham DFT by decomposing ΔE_{int} into classical electrostatic attraction (ΔV_{elstat}), Pauli repulsive orbital interactions between same-spin electrons (ΔE_{Pauli}), and the (mainly electron-pair) bonding orbital interactions (ΔE_{oi}).[21] As pointed out above, the latter can be symmetry decomposed into contributions from

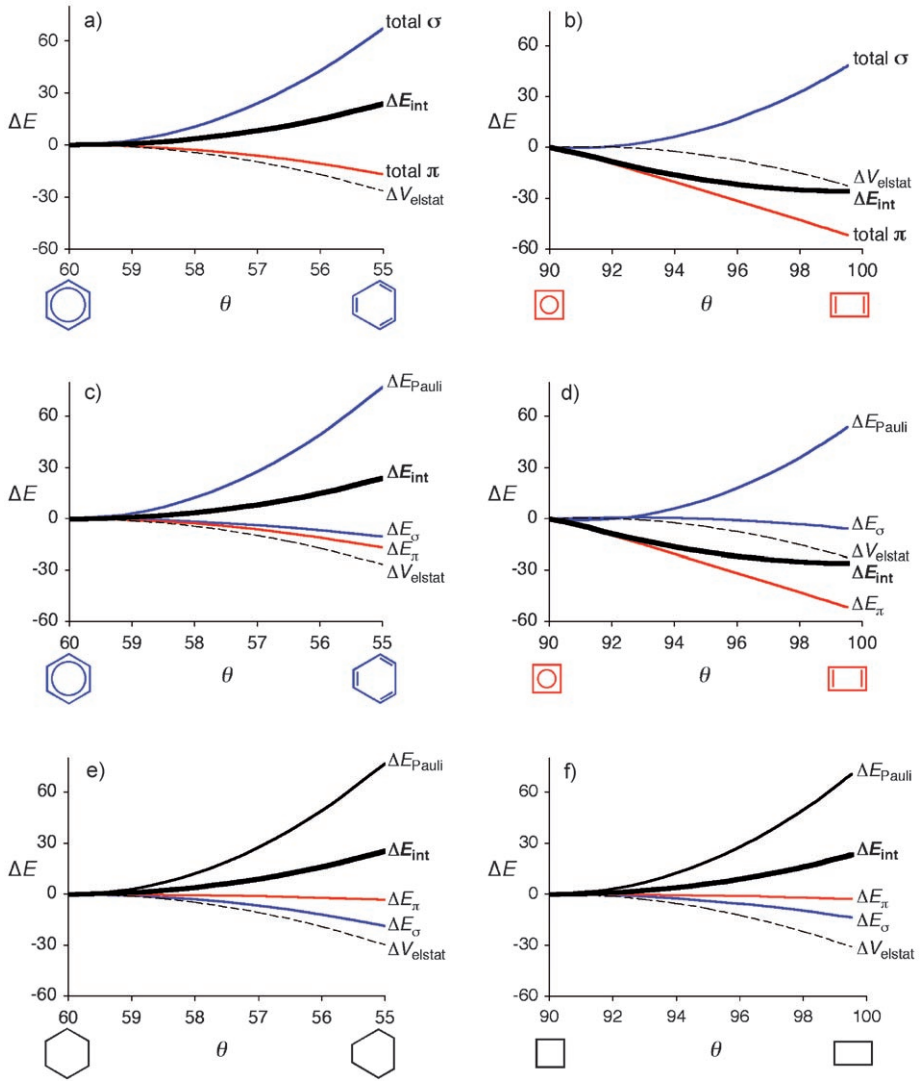

Figure 1. Bond-energy decomposition (kcal mol^{-1}) of **1**, **2**, **3**, and **4**, each constructed from two equivalent rigid fragments, as a function of the distortion mode (°) from delocalized to localized structure as defined for **1** and **2** in Scheme 1. $\Delta E_{int} = (\Delta E_{Pauli} + \Delta E_{o}) + (\Delta E_{\pi}) + \Delta V_{elstat} = (\text{total } \sigma) + (\text{total } \pi) + \Delta V_{elstat}$ computed at BP86/TZ2P.

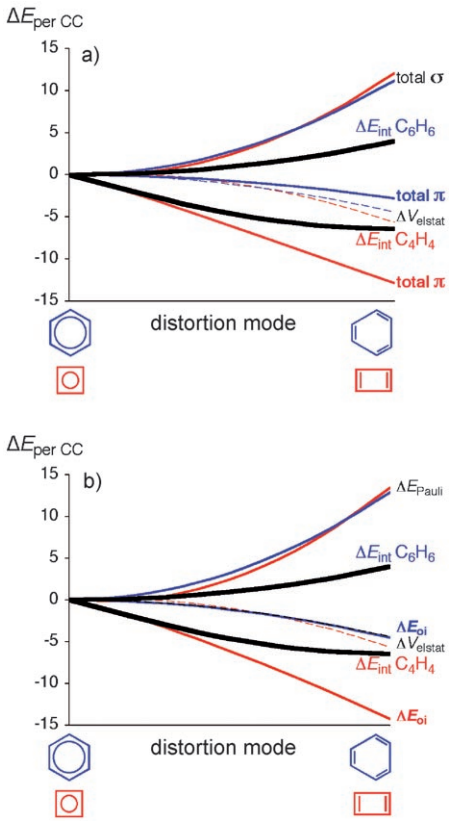

Figure 2. Bond-energy decomposition (kal mol^{-1}) divided by the number of C–C bonds of **1** and **2** superimposed, each constructed from two equivalent rigid fragments, as a function of the distortion mode from delocalized to localized structure as defined in Scheme 1. $\Delta E_{int}=(\Delta E_{Pauli}+\Delta E_{\sigma})+(\Delta E_{\pi})+\Delta V_{elstat}=(\text{total }\sigma)+(\text{total }\pi)+\Delta V_{elstat}$ computed at BP86/TZ2P.

the σ- and π-orbital interactions: $\Delta E_{oi}=\Delta E_{\sigma}+\Delta E_{\pi}$.[14,15] Thus, we have Equation (4):

$$\Delta E_{int} = \Delta E_{Pauli}+\Delta E_{\sigma}+\Delta E_{\pi} +\Delta V_{elstat} \quad (4)$$

Furthermore, because in our construction of **1** and **2** the π electrons contribute no Pauli repulsion (see below), we can write Equation (5):

$$\Delta E_{int} = \text{“total }\sigma\text{”}+\text{“total }\pi\text{”} +\Delta V_{elstat} \quad (5)$$

in which “total σ” $=\Delta E_{Pauli}+\Delta E_{\sigma}$ and “total π” $=\Delta E_{\pi}$.

The results of our analyses, in Figures 1 and 2, show that indeed it is the π electrons that determine if an aromatic, delocalized geometry occurs or an antiaromatic one with localized double bonds. Table 1 provides the full numerical details of the formation of **1** and **2** from CH‴ radicals as well as the overall change in interactions along the localization modes of Scheme 1. In the first place, not unexpectedly, the energy of D_{6h} symmetric benzene (**1**) rises upon localization, whereas localization of the D_{4h} symmetric arrangement of cyclobutadiene towards **2** is accompanied by a stabilization (black bold curves in Figure 1a,b). Now it appears that the σ-electron system always (i.e., in **1** as well as **2**) opposes this localization, whereas the π-electron system always promotes the very same localization of double bonds (compare blue “total σ” with red “total π” curves in Figure 1a,b).

Interestingly, there is a marked difference between the localizing force that the respective π-electron systems exert on the ring geometry in **1** and **2**. In the antiaromatic ring system, the propensity of the π system to localize the double bonds is dramatically increased relative to the aromatic ring (compare red “total π” curve in Figure 1a with that in Figure 1b). This becomes even clearer if we convert ΔE_{int} and its components into energies per C–C bond (or, which is equivalent, per π electron) and superimpose the resulting diagrams of **1** and **2** in Figure 2a. Here we can see that the

Table 1. Bond-energy decomposition [kcal mol^{-1}] of benzene (**1**) and 1,3-cyclobutadiene (**2**) constructed from two $(CH‴)_3$ and two $(CH‴)_2$ fragments, respectively, and bond-energy decomposition of the latter fragments constructed from a corresponding number of CH‴ triradicals.[a]

	Benzene		1,3-Cyclobutadiene	
	1	Δ(**1**→loc)[b]	**2**	Δ(deloc→**2**)[b]
Step 1	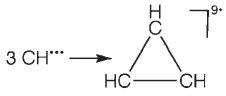		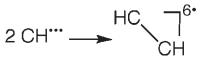	
ΔE_{prep}	0.12	0	0.10	0
ΔE_{σ}	−22.32	0	−19.78	0
ΔE_{π}	−2.85	0	−2.63	0
$\Delta E_{oi}=\Delta E_{\sigma}+\Delta E_{\pi}$	−25.17	0	−22.41	0
ΔE_{Pauli}	105.67	0	82.59	0
ΔV_{elst}	−33.43	0	−22.34	0
$\Delta E_{int}=\Delta V_{elst}+\Delta E_{Pauli}+\Delta E_{oi}$	47.09	0	37.84	0
$\Delta E_{step1}=\Delta E_{prep}+\Delta E_{int}$	47.21	0	37.94	0
Step 2	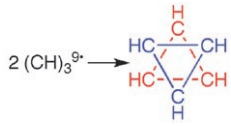		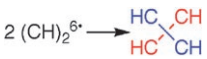	
ΔE_{prep}	0.00	0.00	0.00	0.00
ΔE_{σ}	−1258.27	−10.28	−747.31	−5.55
ΔE_{π}	−210.86	−16.78	−108.53	−51.51
$\Delta E_{oi}=\Delta E_{\sigma}+\Delta E_{\pi}$	−1469.14	−27.06	−855.84	−57.06
ΔE_{Pauli}	1259.58	77.51	665.34	53.82
ΔV_{elst}	−855.64	−26.50	−438.32	−22.51
$\Delta E_{int}=\Delta V_{elst}+\Delta E_{Pauli}+\Delta E_{oi}$	−1065.18	23.95	−628.83	−25.75
$\Delta E_{step2}=\Delta E_{prep}+\Delta E_{int}$	−1065.18	23.95	−628.83	−25.75
Step 1+2	$6\,CH‴\rightarrow C_6H_6$		$4\,CH‴\rightarrow C_4H_4$	
$\Delta E=2\Delta E_{step1}+\Delta E_{step2}$	−970.76	23.95	−552.95	−25.75

[a] Computed at BP86/TZ2P. [b] loc = localized geometry; deloc = delocalized geometry, defined in Scheme 1.

tendency per σ electron to resist localization is essentially equal in **1** (blue curves) and **2** (red curves). Likewise, the classical electrostatic attraction ΔV_{elstat}, which slightly favors localization, is essentially equal in **1** and **2**. The discriminating factor is the tendency per π electron to localize the geometry, which is about three times larger in the antiaromatic species (**2**) than in the aromatic one (**1**). Similar results are obtained for the alternative distortions that were presented earlier in the manuscript.

How can we understand the above? The σ bonds are characterized by an equilibrium distance greater than zero, roughly 1.5 Å for C–C bonds. One reason for this is the early onset of $<2p_\sigma|2p_\sigma'>$ relative to $<2p_\pi|2p_\pi'>$ overlap, and the fact that the former achieves an optimum at distances greater than zero, whereas the latter is maximal at distance zero (see also Ref. [23]). This is illustrated in Figure 3

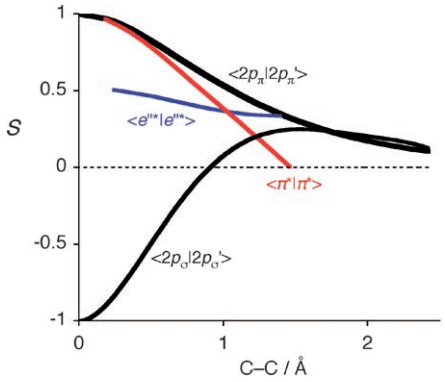

Figure 3. Selected overlap integrals (S) between MOs of two $CH^{\bullet\bullet\bullet}$ units in **1** (black curves), between MOs of two $(CH)_3^{9\bullet}$ units in **1** (blue curve), and between two $(CH)_2^{6\bullet}$ units in **2** (red curve) as a function of the C–C distance along the localization distortion defined in Scheme 1.

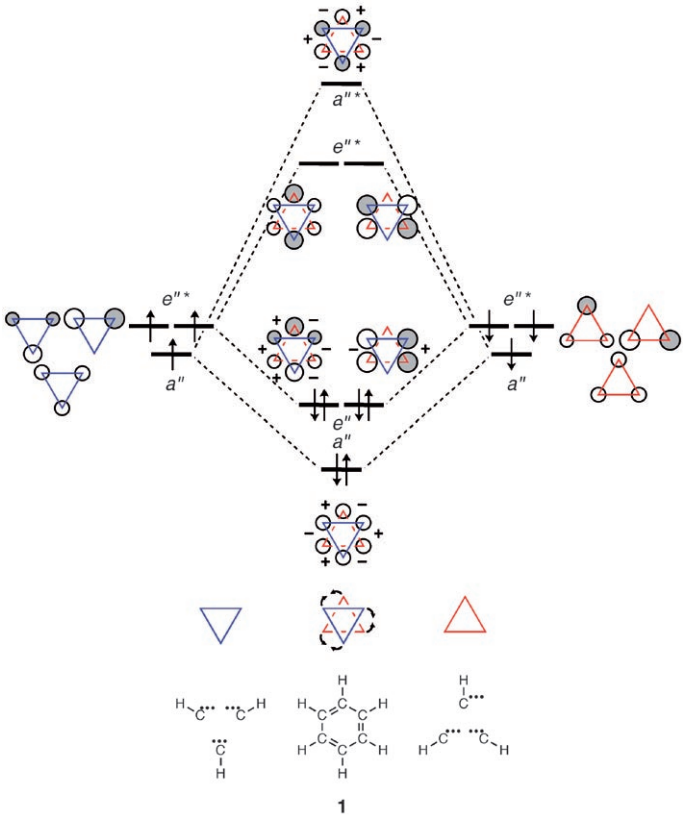

Figure 4. Schematic π MO interaction diagram of benzene (**1**) constructed from two $(CH)_3^{9\bullet}$ fragments in their decet valence configuration, based on Kohn–Sham MO analyses at BP86/TZ2P. There are 3 π electrons in each of the two fragments, which have mutually opposite spin. The effect on orbital energies of the localization mode defined in Scheme 1 and represented here with curved arrows is indicated by + (stabilization) and − (destabilization).

for two $C–H^{\bullet\bullet\bullet}$ fragments in benzene approaching each other on localization (see black curves). However, as pointed out before in a different context,[24] the main reason for σ bonds to feature an optimum distance greater than zero is the repulsive wall provided by Pauli repulsion with the closed shell 2*s* (and 1*s*) atomic orbitals (AO) on carbon and the C–H bonds. In the symmetric, delocalized structures of benzene and cyclobutadiene, each C–C bond is already forced by partial π bonding below the optimum σ distance, that is, it is already in the region in which the Pauli repulsion ΔE_{Pauli} due to the σ electrons increases in energy faster than the stabilizing orbital interactions ΔE_σ and ΔV_{elstat} together decrease. This becomes clear if one separates "total σ", shown in Figure 1a,b and Figure 2a, into its component $\Delta E_{\text{Pauli}} + \Delta E_\sigma$ as has been done in Figure 1c,d and Figure 2b.

The π-electron systems, on the other hand, provide only electron-pair bonding and no Pauli repulsive orbital interactions, as can be seen in Figures 4 and 5. They achieve an optimum overlap at zero bond length (see Figure 3). But why is the localizing propensity of the π system in **1** so little pronounced although it is so prominent in **2**? Essential for understanding this difference is the qualitatively different topology and geometry dependence of the π overlaps in our aromatic and antiaromatic 6 and 4 π-electron systems compared to a simple 2 π-electron system, represented by the black $<2p_\pi|2p_\pi'>$ curve in Figure 3. Scheme 2 extracts from Figures 4 and 5 the key features that emerge from our quantitative Kohn–Sham MO analyses.

The main difference between π overlap in **1** and **2** versus that between two simple $CH^{\bullet\bullet\bullet}$ fragments is the occurrence of counteracting effects, on localization, in **1** and amplifying effects in **2**. Whereas the $<2p_\pi|2p_\pi'>$ overlap between two $CH^{\bullet\bullet\bullet}$ fragments smoothly increases from 0 (at $C–C=\infty$) towards the value 1 (at $C–C=0$), the π bonding a'' MOs in both **1** and **2** gain and loose bonding overlap in the shrinking and expanding C–C bonds, respectively (see Figure 3; see also Figures 4 and 5). Eventually, the net effect is still a gain in bonding, but in essence this is not so pronounced anymore (see Scheme 2). The same holds for the π-bonding set of degenerate e'' MOs in **1** (see Scheme 2: stabilizing and destabilizing effects are indicated for one of these e'' MOs with + and − signs, respectively). This makes benzene's π system relatively indifferent with respect to localizing the double C–C bonds.

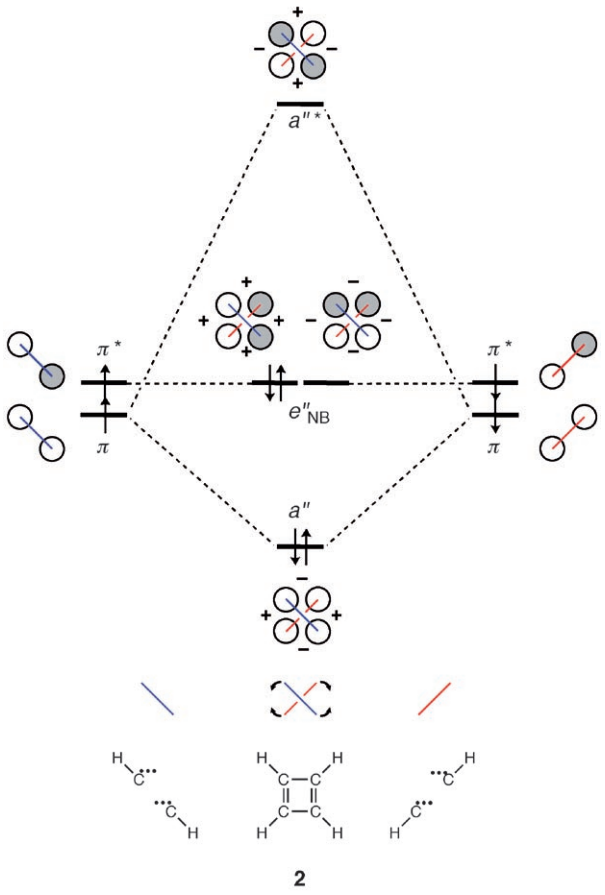

Figure 5. Schematic π MO interaction diagram of 1,3-cyclobutadiene (**2**) constructed from two $(CH)_3^{6\bullet}$ fragments in their septet valence configuration, based on Kohn–Sham MO analyses at BP86/TZ2P. There are 2 π electrons in each of the two fragments, which have mutually opposite spin. The effect on orbital energies of the localization mode defined in Scheme 1 and represented here with curved arrows is indicated by + (stabilization) and − (destabilization).

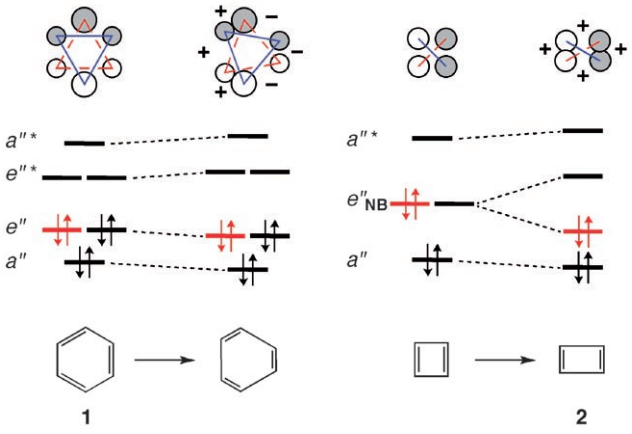

Scheme 2. Effect of localization on π MO levels of **1** and **2**. Orbital plots at top refer to red levels.

A completely different situation holds for the nonbonding degenerate e''_{NB} MOs in the second-order Jahn–Teller unstable D_{4h} symmetric geometry of cyclobutadiene.[23] One of these π MOs gains, on localization, stabilization in every C–C bond (this is indicated with the + signs in Scheme 2). And it does so rapidly. This is because the orbital overlap starts to build up from 0 (i.e., no overlap and no stabilization) at a short C–C distance of 1.465 Å and rises to the value 1 as the C–C distance decreases to 0 (see Figure 3). This differs from the distance dependence of the π overlap between two $2p_\pi$ AOs on two simple $CH^{\bullet\bullet\bullet}$ fragments (or on two carbon atoms) that has its zero point at a C–C distance of ∞, but also goes to 1 as the C–C distance decreases to 0 Å (see $<2p_\pi|2p_\pi'>$ in Figure 3). Along the bond-localizing distortion, the gain in overlap between the two π* $(CH)_2^{6\bullet}$ fragment MOs (shown in Figure 5) is a sizeable 0.102! (see Figure 3). (The corresponding gain in overlap between two e''^* $(CH)_3^{9\bullet}$ fragment MOs that form a π-bonding e'' MO in benzene (shown in Figure 4) amounts to only 0.003.) As a consequence, this cyclobutadiene MO, which is fully occupied in the singlet ground state of **2**, drops markedly in energy along the localization mode. This lends cyclobutadiene's π system its enhanced propensity towards localization of the C=C double bonds.

Finally, it is instructive to compare the aromatic **1** and antiaromatic **2** with the corresponding saturated nonaromatic **3** and **4**. For clarity and comparability, this is done for planar **3** and **4**, which are 24.5 and 0.9 kcal mol^{-1} above the chair and puckered-ring equilibrium conformations, respectively. The latter are obtained from **1** and **2** by saturating the double bonds with hydrogen that occupies the antibonding π orbitals. For the six-membered ring, the transformation of **1** to **3** has relatively little effect. Of course, the C–C bonds expand (from 1.398 to 1.557 Å) as the net π bonding vanishes. However, the regular, delocalized structure remains as it was determined by the σ system, which is practically unchanged. This is illustrated by our quantitative bond-energy decomposition of **3** and **4** constructed in analogy to **1** and **2** from two $(CH_2)_3^{6\bullet}$ or two $(CH_2)_2^{4\bullet}$ fragments. Indeed there are relatively few changes from **1** to (planar) **3**: the most important one is that the small ΔE_π term of **1** becomes even smaller in **3** (see Figure 1c,e). In the case of the four-membered ring, the changes from **2** to **4** are more drastic. Here, saturation of the double bonds eliminates the strongly localizing π-bonding component which, as a consequence, can no longer overrule the delocalizing σ system. Thus, the latter causes **4** to adopt a regular structure with four equal C–C bonds of 1.559 Å. This is clearly seen by comparing Figure 1d and f, in which the main change is the collapse of the ΔE_π component.

Conclusions

Our MO model of aromaticity augments and confirms the modern VB picture developed by Shaik and Hiberty. This MO model shows that indeed the π-electron system never favors a symmetric, delocalized ring, neither in benzene (**1**) nor in cyclobutadiene (**2**). The regular, symmetric structure

of benzene has the same cause as that of planar cyclohexane (**3**), namely, the σ-electron system. Yet, the π system decides if delocalization occurs by showing qualitatively different geometry dependence of the π overlap in **1** and **2**. In the aromatic species, the localizing propensity of the π system emerges from a subtle interplay of counteracting overlap effects and is, therefore, too little pronounced to overcome the delocalizing σ system. At variance, in the antiaromatic ring, all π-overlap effects unidirectionally favor localization of the double bonds and can, in this way, overrule the σ system.

Acknowledgements

We thank the Netherlands Organization for Scientific Research (NWO-CW and NWO-NCF) for financial support.

[1] a) A. Kekulé, *Bull. Soc. Chim. Paris* **1865**, 3, 98; b) Benzene was first isolated by Faraday: M. Faraday, *Philos. Trans. R. Soc. London* **1825**, 440.
[2] a) P. J. Garratt, *Aromaticity*, John Wiley & Sons, New York, **1986**; b) V. I. Minkin, M. N. Glukhotsev, B. Y. Simkin, *Aromaticity and Antiaromaticity: Electronic and Structural Aspects*, John Wiley & Sons, New York, **1994**; c) F. Bickelhaupt, W. H. de Wolf, *Recl. Trav. Chim. Pays-Bas* **1988**, *107*, 459; d) P. A. Kraakman, J.-M. Valk, H. A. G. Niederländer, D. B. E. Brouwer, F. M. Bickelhaupt, W. H. de Wolf, F. Bickelhaupt, C. H. Stam, *J. Am. Chem. Soc.* **1990**, *112*, 6638.
[3] P. von R. Schleyer, H. J. Jiao, *Pure Appl. Chem.* **1996**, *68*, 209.
[4] F. A. Carey, R. J. Sundberg, *Advanced Organic Chemistry: Structure And Mechanisms (Part A)*, Springer, New York, **2000**.
[5] Special issue on "Aromaticity" (Guest ed.: P. von R. Schleyer), *Chem. Rev.* **2001**, *101*, issue 5.
[6] Special issue on "Delocalization—Pi and Sigma" (Guest ed.: P. von R. Schleyer), *Chem. Rev.* **2005**, *105*, issue 10.
[7] a) R. Breslow, *Acc. Chem. Res.* **1973**, *6*, 393; b) T. M. Krygowski, M. K. Cyranski, Z. Czarnocki, G. Hafelinger, A. R. Katritzky, *Tetrahedron* **2000**, *56*, 1783; c) P. von R. Schleyer, *Chem. Rev.* **2001**, *101*, 1115; d) M. K. Cyranski, T. M. Krygowski, A. R. Katritzky, P. von R. Schleyer, *J. Org. Chem.* **2002**, *67*, 1333.
[8] a) L. Pauling, *J. Am. Chem. Soc.* **1926**, *48*, 1132; b) L. Pauling, *The Nature of the Chemical Bond*, 3rd ed., Cornell University Press, New York, **1960**.
[9] E. Hückel, *Z. Phys.* **1931**, 70, 204.
[10] M. J. Goldstein, R. Hoffmann, *J. Am. Chem. Soc.* **1971**, *93*, 6193.
[11] a) P. C. Hiberty, S. S. Shaik, J. M. Lefour, G. Ohanessian, *J. Org. Chem.* **1985**, *50*, 4657; b) S. S. Shaik, P. C. Hiberty, *J. Am. Chem. Soc.* **1985**, *107*, 3089; c) P. C. Hiberty, S. S. Shaik, G. Ohanessian, J. M. Lefour, *J. Org. Chem.* **1986**, *51*, 3908; d) S. S. Shaik, P. C. Hiberty, J. M. Lefour, G. Ohanessian, *J. Am. Chem. Soc.* **1987**, *109*, 363; e) S. S. Shaik, P. C. Hiberty, G. Ohanessian, J. M. Lefour, *J. Phys. Chem.* **1988**, *92*, 5086; f) P. C. Hiberty, D. Danovich, A. Shurki, S. Shaik, *J. Am. Chem. Soc.* **1995**, *117*, 7760; g) A. Shurki, S. Shaik, *Angew. Chem.* **1997**, *109*, 2322; *Angew. Chem. Int. Ed. Engl.* **1997**, *36*, 2205; h) S. Shaik, A. Shurki, D. Danovich, P. C. Hiberty, *Chem. Rev.* **2001**, *101*, 1501.
[12] a) F. Dijkstra, J. H. van Lenthe, R. W. A. Havenith, L. W. Jenneskens, *Int. J. Quantum Chem.* **2003**, 91, 566; b) Y. R. Mo, P. von R. Schleyer, *Chem. Eur. J.* **2006**, *12*, 2009.
[13] I. Fernández, G. Frenking, *Faraday Discuss.* **2007**, *135*, 403.
[14] a) Y. Ooshika, *J. Phys. Soc. Japan* **1957**, *12*, 1238; b) H. Labhart, *J. Chem. Phys.* **1957**, *27*, 947; c) H. C. Longuet-Higgins, L. Salem, *Proc. R. Soc. London Ser. A* **1959**, *251*, 172; d) M. Tsui, S. Huzinaga, T. Hasino, *Rev. Mod. Phys.* **1960**, 32, 425; e) R. S. Berry, *J. Chem. Phys.* **1961**, *35*, 2253.
[15] a) Y. Haas, S. Zilberg, *J. Am. Chem. Soc.* **1995**, *117*, 5387; b) E. Heilbronner, *J. Chem. Educ.* **1989**, *66*, 471; c) A. Stanger, K. P. C. Vollhardt, *J. Org. Chem.* **1988**, *53*, 4889; d) N. D. Epiotis, *Pure Appl. Chem.* **1983**, *55*, 229.
[16] W. Kutzelnigg, *Einführung in die Theoretische Chemie, Band 2, Die chemische Bindung*, Verlag Chemie, Weinheim, **1978**, Section 11.11.
[17] a) N. C. Baird, *J. Org. Chem.* **1986**, *51*, 3907; b) E. D. Glendening, R. Faust, A. Streitwieser, K. P. C. Vollhardt, F. Weinhold, *J. Am. Chem. Soc.* **1993**, *115*, 10952.
[18] a) K. Jug, A. M. Koster, *J. Am. Chem. Soc.* **1990**, *112*, 6772; b) A. Gobbi, Y. Yamaguchi, G. Frenking, H. F. Schaefer III, *Chem. Phys. Lett.* **1995**, *244*, 27; c) B. Kovacevic, D. Baric, Z. B. Maksic, T. Müller, *ChemPhysChem* **2004**, *5*, 1352; d) A. Rehaman, A. Datta, S. S. Mallajosyula, S. K. Pati, *J. Chem. Theory Comput.* **2006**, *2*, 30.
[19] a) R. Hoffmann, *Angew. Chem.* **1982**, *94*, 725; *Angew. Chem. Int. Ed. Engl.* **1982**, *21*, 711; b) For an instructive discussion on the pros and cons of MO versus VB theory, see: R. Hoffmann, S. Shaik, P. C. Hiberty, *Acc. Chem. Res.* **2003**, *36*, 750.
[20] a) G. te Velde, F. M. Bickelhaupt, S. J. A. van Gisbergen, C. Fonseca Guerra, E. J. Baerends, J. G. Snijders, T. Ziegler, *J. Comput. Chem.* **2001**, *22*, 931; b) C. Fonseca Guerra, O. Visser, J. G. Snijders, G. te Velde, E. J. Baerends in *Methods and Techniques for Computational Chemistry* (Eds.: E. Clementi, G. Corongiu), STEF: Cagliari, 1995, pp. 305; c) E. J. Baerends, D. E. Ellis, P. Ros, *Chem. Phys.* **1973**, *2*, 41; d) E. J. Baerends, P. Ros, *Chem. Phys.* **1975**, *8*, 412; e) E. J. Baerends, P. Ros, *Int. J. Quantum Chem. Symp.* **1978**, *12*, 169; f) C. Fonseca Guerra, J. G. Snijders, G. te Velde, E. J. Baerends, *Theor. Chem. Acc.* **1998**, *99*, 391; g) P. M. Boerrigter, G. te Velde, E. J. Baerends, *Int. J. Quantum Chem.* **1988**, *33*, 87; h) G. te Velde, E. J. Baerends, *J. Comp. Phys.* **1992**, *99*, 84; i) J. G. Snijders, E. J. Baerends, P. Vernooijs, *At. Nucl. Data Tables* **1982**, *26*, 483; j) J. Krijn, E. J. Baerends, *Fit-Functions in the HFS-Method; Internal Report (in Dutch)*, Vrije Universiteit, Amsterdam, **1984**; k) L. Versluis, T. Ziegler, *J. Chem. Phys.* **1988**, *88*, 322; l) J. C. Slater, *Quantum Theory of Molecules and Solids, Vol. 4*, McGraw-Hill, New York, **1974**; m) A. D. Becke, *J. Chem. Phys.* **1986**, *84*, 4524; n) A. Becke, *Phys. Rev. A* **1988**, *38*, 3098; o) S. H. Vosko, L. Wilk, M. Nusair, *Can. J. Phys.* **1980**, *58*, 1200; p) J. P. Perdew, *Phys. Rev. B* **1986**, *33*, 8822; corrigendum *Phys. Rev. B* **1986**, *34*, 7406; q) L. Fan, T. Ziegler, *J. Chem. Phys.* **1991**, *94*, 6057.
[21] a) F. M. Bickelhaupt, E. J. Baerends in *Rev. Comput. Chem. Vol. 15*, **2000**, pp. 1; b) F. M. Bickelhaupt, N. M. M. Nibbering, E. M. van Wezenbeek, E. J. Baerends, *J. Phys. Chem.* **1992**, *96*, 4864; c) T. Ziegler, A. Rauk, *Inorg. Chem.* **1979**, *18*, 1755; d) T. Ziegler, A. Rauk, *Inorg. Chem.* **1979**, *18*, 1558; e) T. Ziegler, A. Rauk, *Theor. Chim. Acta* **1977**, *46*, 1.
[22] K. Morokuma, *Acc. Chem. Res.* **1977**, *10*, 294.
[23] T. A. Albright, J. K. Burdett, M.-H. Whangbo, *Orbital Interactions in Chemistry*, John Wiley & Sons, New York, **1985**.
[24] a) F. M. Bickelhaupt, E. J. Baerends, *Angew. Chem.* **2003**, *115*, 4315; *Angew. Chem. Int. Ed.* **2003**, *42*, 4183; b) F. M. Bickelhaupt, R. L. DeKock, E. J. Baerends, *J. Am. Chem. Soc.* **2002**, *124*, 1500.

Received: February 5, 2007
Published online: June 19, 2007

